



Improving the cutting quality of aluminum alloy machined by abrasive waterjet with a relatively low pressure

Shuo Sun^{1,2} · Yi'nan Qian^{1,2} · Wenjun Lu^{1,2} · Shijing Wu^{1,2} · Yong Kang^{1,2} · Aili Tan³ · Deng Li^{1,2} 

Received: 30 December 2022 / Accepted: 13 June 2023 / Published online: 24 June 2023
© The Author(s), under exclusive licence to The Brazilian Society of Mechanical Sciences and Engineering 2023

Abstract

The cutting quality of abrasive waterjet (AWJ) can be generally improved by increasing the pressure, but a higher pressure means a reduced service life of the equipment and increased manufacturing and maintenance cost. In order to obtain the required high cutting quality at a relatively low pressure of 150 MPa, the process parameters of AWJ were optimized using the response surface methodology (RSM). The surface roughness (R_a) and the kerf taper (K_t) were used to evaluate the cutting quality. The Central Composite Design (CCD) model was applied for designing the cutting experiment, and the effects of abrasive flow rate, standoff distance, and traverse speed on the machining quality were analyzed using the method of Analysis of Variance (ANOVA). By using the obtained optimal machining parameters of AWJ, the double-pass strategy was used to further promote the cutting quality. The results show that the cutting quality at the low pressure of 150 MPa can be significantly improved by optimizing the process parameters or increasing the number of cutting pass. The highest cutting quality of $R_a = 4.55 \mu\text{m}$ and $K_t = 0.149^\circ$ can be achieved at a traverse speed of 33 mm/min, a standoff distance of 0.66 mm, and an abrasive flow rate of 339 g/min. Using the strategy of double-pass cutting, the R_a can be reduced by a maximum of 82.74%, and the greatest reduction in K_t is 59.94%, meaning the cutting quality is better when compared with that under the ultra-high pressure of 350 MPa with single-pass cutting.

Keywords Abrasive waterjet · Low pressure · Response surface methodology · Surface roughness · Kerf taper

1 Introduction

Abrasive waterjet (AWJ) is a non-traditional green machining method being widely used in the world today. AWJ is formed by adding abrasive particles into the high-speed water beam, and the material removal is mainly achieved by the shearing effect of abrasive particles [1]. This technology is able to machine a wide range of materials because of its unique advantages like higher versatility, no heat affected zone, lower cutting forces, and good environmental

performance [2]. During its working process, nearly no dust or harmful particles are produced, which is friendly to the environment [3]. The performance of AWJ processing is affected by various parameters, among which the waterjet pressure, the abrasive flow rate, the traverse speed, and the standoff distance are the main ones [4].

In order to improve the cutting ability of AWJ, many researchers are focusing on investigating the effects of machining parameters on the roughness (R_a) and taper (K_t) of the cut surface and kerf. For example, Arvind et al. [5] experimentally studied the influence of AWJ processing parameters on the cutting quality of Inconel 718 with the use of response surface methodology (RSM). They found that both the abrasive flow rate and traverse speed are the most substantial parameters. Similar results were also obtained by Joel et al. [6], who used the Taguchi method linked with the gray relation analysis to investigate the machinability of AA7075 aluminum alloy by AWJ. Moreover, Ahmed et al. [7] used experimental design and statistical modeling techniques to make an investigation on the influence of AWJ cutting parameters on the surface roughness. As a result, the

Technical Editor: Lincoln Cardoso Brandao.

✉ Deng Li
2008lee@whu.edu.cn

¹ Hubei Key Laboratory of Waterjet Theory and New Technology, Wuhan University, Wuhan 430072, China

² School of Power and Mechanical Engineering, Wuhan University, Wuhan 430072, China

³ Department of Gynecology, Renmin Hospital of Wuhan University, Wuhan 430060, China

waterjet pressure and traverse speed were claimed as significant parameters. Yuvaraj et al. [8] studied the cutting performance of cryogenic-assisted AWJ under different waterjet pressures, abrasive sizes, and AWJ impact angles. Xiong et al. [9] put forward a new cutting strategy that reverses cutting with variable standoff distance to improve the cutting performance of Ti6Al4V. Besides, Yang et al. [10] studied the effects of processing parameters on the cutting capacity and quality with the monolithic abrasive material and corresponding mixing abrasive materials, respectively. They found that the variation of abrasive flow rate greatly determines the cutting performance. These investigations indicate that by optimizing the machining parameters of AWJ, the cutting quality of materials can be significantly improved.

On the other hand, numerous studies in the literature have already shown that waterjet pressure is one of the most significant factors affecting the cutting ability of AWJ and the cutting quality [11–13]. It can be claimed that a higher waterjet pressure generally results in better cutting qualities, especially for hard materials [14, 15]. Our previous cutting experiments also showed that the waterjet pressure should be as high as 400 MPa when cutting U71Mn material if satisfied surface quality needs to be obtained [16]. Therefore, experiments and investigations are mainly performed at ultra-high pressures. Almost all, the studies on AWJ cutting are conducted at pressures above 300 MPa, and so far, few investigations on AWJ cutting at pressures below 200 MPa can be found in the literature. But it is known that a higher pump pressure means that the manufacturing and maintenance cost will be largely raised and the service life will be greatly reduced at the same time [17]. Up to now, whether a relatively low pressure waterjet can cut materials with a high quality as that achieved by ultra-high pressure waterjets remains unclear.

In the present study, an attempt was made to discover the cutting ability of AWJ with a relatively low pressure. By varying the traverse speed, standoff distance, abrasive flow rate, and the number of cutting pass, the cutting quality of 5052 aluminum alloy under the impact of AWJ at 150 MPa was studied. The cutting quality was then compared with an ultra-high pressure of 350 MPa. This study could help obtain a high cutting quality of AWJ at a low waterjet pressure by using reasonable machining parameters.

2 Experimental procedure and facilities

2.1 Specimen

As aluminum alloy 5052 has superior manufacturability such as formability, corrosion resistance, and weldability, it is being widely employed in aircraft fuel tanks, autonomous body structures, and sheet metal parts of marines [18]. Thus, aluminum alloy 5052 was used as the cutting specimen in this study, and the chemical composition and main mechanical properties are displayed in Tables 1 and 2, respectively [19, 20]. The dimensions of length, width, and thickness of the specimen were 20 mm, 10 mm, and 5 mm, respectively.

2.2 Equipment

All the cutting tests were performed using an AWJ platform (Model: APW2016BA-18) shown in Fig. 1. The platform was equipped with a five-axis cutting head and a pump with the maximum ultra-high pressure up to 420 MPa. The AWJ device also had an abrasive delivery system that can adjust the abrasive flow rate ranging from 70 to 880 g/min.

The roughness of the cut surface, R_a , was obtained by the contact-type surface measuring instrument (Mitutoyo SJ-210). Three different locations on the surface of each specimen were selected for measurement, and the average values were used to minimize the errors. The measurement length was 6 mm, and the movement speed of the probe was 0.5 mm/s. The calculation results and surface roughness waveform can be displayed on the device. The instrument and measurement method are shown in Fig. 2.

The taper of the cut kerf, K_t , was also used for evaluating the quality of the cut surface, and it was obtained by a three-dimensional profiler (Model: NanoFocus μ scan) illustrated in Fig. 3. The profiler was used to collect the contour shape of the cut surface and measure the width of the upper and lower cuts. Then, K_t could be obtained using the following equation [21]

Table 2 Main mechanical properties of aluminum alloy 5052

Density (g/cm ³)	Tensile strength (MPa)	Yield strength (MPa)	Thermal conductivity (W/mK)	Elastic Modulus (GPa)
2.7	220	65	121	70

Table 1 Chemical composition of aluminum alloy 5052

Si%	Cu%	Mg%	Zn%	Mn%	Cr%	Fe%	Al%
≤0.25	≤0.10	2.2~2.8	≤0.10	≤0.10	0.15~0.35	≤0.40	Bal

Fig. 1 AWJ devices

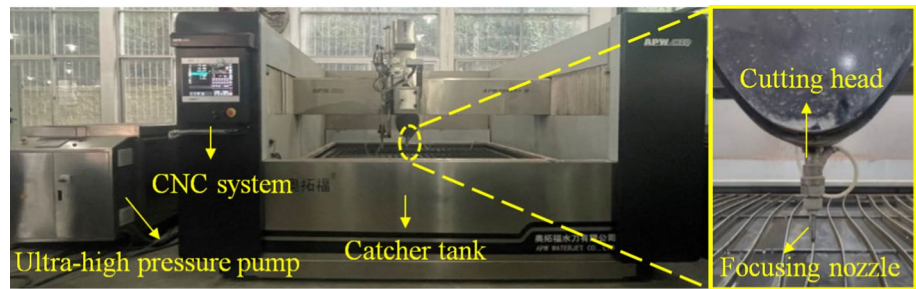


Fig. 2 Mitutoyo SJ-210 and measurement method

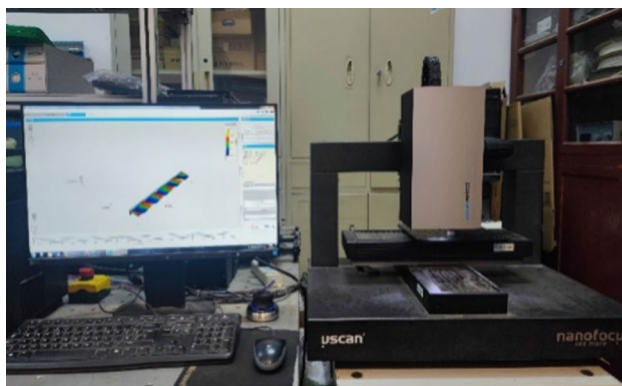
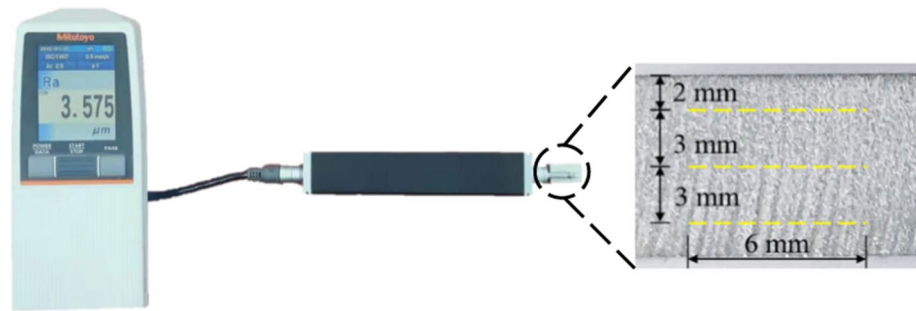


Fig. 3 NanoFocus μscan profiler

$$K_t = \tan^{-1} \left(\frac{W_t - W_b}{2h} \right) \tag{1}$$

where W_t , W_b , and h are, respectively, denoted as the width of the upper kerf, the width of the lower kerf, and the thickness of the specimen.

2.3 Experimental design

During all the cutting tests, the waterjet impact angle, the garnet abrasive size, and the focusing nozzle diameter were kept as 90° , 80 mesh, and 1.02 mm, respectively. Preliminary cutting experiments had been performed, and results showed that 150 MPa was the minimum pressure for cutting through the aluminum alloy 5052 specimen at a single cutting. In the meantime, a relatively high cutting quality

of $R_a = 4.842 \mu\text{m}$ and $K_t = 1.118^\circ$ could be obtained at a much higher pressure of 350 MPa with the traverse speed of 100 mm/min, standoff distance of 2 mm, and abrasive flow rate of 390 g/min. Thus, 150 MPa was used as the relatively low pressure, and 350 MPa was used as the ultra-high pressure for comparison.

In this study, two cutting methods were used to improve the machining quality at the relatively low pressure of 150 MPa. One was optimizing the main process parameters, which were the traverse speed, the standoff distance, and the abrasive flow rate, the other was using double-pass cutting with alternate directions.

RSM, which is a statistical method for solving multivariate problems, was used in company with the Central Composite Design (CCD) model. One advantage of CCD over Box-Behnken Design (BBD) and other design techniques of the experiment is its design flexibility, which allows for increased factor levels by adding axial points [22]. In general, the basic form of the multivariate quadratic response surface regression model is shown as follows [23].

$$Y = b_0 + \sum_{i=1}^{\infty} b_i X_i + \sum_{i=1}^{\infty} b_{ii} X_i^2 + \sum_{i=1}^{\infty} \sum_{j>1}^{\infty} b_{ij} X_i X_j + \epsilon \tag{2}$$

where Y is the response factor (R_a , K_t), b_0 is the regression intercept, b_i , b_{ii} , and b_{ij} are regression coefficients, ϵ is the random experimental error, and X_i , X_j are independent variables of dimensionless coded.

A model of three factors at five levels was adopted to obtain the optimum cutting parameters. Coding factors A, B, and C stand for the traverse speed, the standoff distance,

and the abrasive flow rate, separately. For each factor, the values of levels 2 and 4 were determined by the preliminary experiment, and the other three levels were acquired by the CCD model. All the process parameters are summarized in Table 3.

3 Results and discussion

A total of 40 cutting tests were performed at the relatively low pressure of 150 MPa. In more specific terms, 20 tests were under single-pass cutting, and the other 20 were under double-pass cutting. The values of R_a and K_t of each test are displayed in Table 4, as well as those obtained at the ultra-high pressure of 350 MPa in the preliminary experiment, for the convenience of comparison.

3.1 Cutting quality improvement by optimizing process parameters

The optimization of the three process parameters was studied under the condition of single-pass cutting. RSM was used for clarifying the influence of process parameters on the response metrics. It also helped to establish the quadratic regression equation models of R_a and K_t considering the above cutting parameters. The final quadratic regression equation models of R_a and K_t according to the coding factors are given in Eqs. 3 and 4, respectively.

$$R_a = 12.59 + 2.32A - 0.7419B - 1.94C - 1.27AC - 1.63A^2 + 0.5473C^2 \tag{3}$$

Table 3 Levels of the cutting parameters in the experiment

Symbol	Input parameters	Level				
		1	2	3	4	5
A	Traverse speed (mm/min)	33	50	75	100	117
B	Standoff distance (mm)	0.66	1	1.5	2	2.34
C	Abrasive flow rate (g/min)	70	200	390	580	710

Table 4 R_a and K_t values at different cutting conditions

Run order	Input parameters			Single-pass cutting		Double-pass cutting	
	Traverse speed	Standoff distance	Abrasive flow rate	R_a	K_t	R_a	K_t
	(mm/min)	(mm)	(g/min)	(μm)	(degree)	(μm)	(degree)
1	75	1.5	390	12.978	1.086	2.979	0.435
2	75	2.34	390	11.585	1.274	3.021	0.871
3	50	1	580	8.821	0.809	2.420	0.528
4	33	1.5	390	4.789	0.590	2.503	0.280
5	75	1.5	710	10.561	1.491	2.626	0.621
6	100	1	580	11.680	1.613	2.593	0.808
7	75	1.5	390	12.976	1.235	2.744	0.839
8	75	1.5	390	12.878	1.182	2.688	0.901
9	50	2	200	8.841	1.056	3.412	0.777
10	75	1.5	70	17.576	0.988	3.590	0.590
11	100	2	200	15.510	1.615	3.406	0.714
12	117	1.5	390	11.003	1.522	3.109	0.776
13	50	2	580	7.846	1.212	2.756	0.746
14	100	1	200	19.126	1.553	3.301	0.870
15	75	0.66	390	13.409	0.809	2.902	0.932
16	75	1.5	390	12.245	1.130	3.005	1.087
17	100	2	580	10.487	1.690	2.774	1.088
18	75	1.5	390	12.435	0.978	3.119	1.025
19	75	1.5	390	12.108	1.119	2.515	0.994
20	50	1	200	10.120	0.641	3.124	0.622
C. g	100	2	390	4.842	1.118		

C. g Control group

$$K_t = 1.13 + 0.3164A + 0.1273B + 0.0955C + 0.0743C^2 \tag{4}$$

However, it should be pointed out that in double-pass cutting, due to the polishing and trimming effects of the secondary cutting, the influence of various factors on cutting quality is weakened, and the prediction model of quadratic regression equation is not reliable. Therefore, only the surface quality prediction model of single-pass cutting is analyzed in this paper.

Analysis of variance (ANOVA), generally used for significance testing, was applied to evaluate the significance of the cutting parameters. The ANOVA analysis result of R_a under 150 MPa single-pass cutting is shown in Table 5. The F-value of the model is 52.71, and the P value is less than 0.05, which indicates that the established model is significant. Each item with p value less than 0.05 has a significant

influence on the model as a whole. As can be seen from Table 5, A, B, C, AC, A^2 , C^2 are the significant model terms. Similarly, the ANOVA result for the K_t of 150 MPa single-pass cutting is shown in Table 6, from which it can be found that the K_t is influenced significantly by the model terms of A, B, C, and C^2 .

The normal plots of residuals of R_a and K_t are shown in Fig. 4. All residuals are approximately evenly distributed along a straight line, indicating that the error of the regression model obtained is small and the accuracy is high. Therefore, it can be used as a basis for predicting the results of response variables [24].

The approximate degree of the actual values and predicted values of R_a and K_t are shown in Fig. 5. The actual values and predicted values are generally distributed near the central line, which has a good linear fitting relationship [25]. This shows the good applicability of the model,

Table 5 ANOVA for R_a

Source	Sum of Squares	DOF	Mean Square	F-value	P-value
Model	193.09	9	21.54	52.71	<0.001
A-Travel speed	73.24	1	73.24	179.94	<0.001
B-Standoff distance	7.52	1	7.52	18.47	0.0016
C-Abrasive flow rate	51.65	1	51.65	126.90	<0.001
AB	0.8162	1	0.8162	2.01	0.1871
AC	12.94	1	12.94	31.79	0.0002
BC	0.9293	1	0.9293	2.28	0.1617
A^2	38.57	1	38.57	94.76	<0.001
B^2	0.0013	1	0.0013	0.0031	0.9565
C^2	4.30	1	4.30	10.57	0.0087
Residual	4.07	10	0.4070		
Lack of fit	3.31	5	0.6628	4.38	0.0654
Pure error	0.7563	5	0.1513		
Cor total	197.16	19			

Table 6 ANOVA for K_t

Source	Sum of Squares	DOF	Mean Square	F-value	P-value
Model	1.86	9	0.2064	12.39	0.0003
A-Travel speed	1.37	1	1.37	82.04	<0.001
B-Standoff distance	0.2213	1	0.2213	13.28	0.0045
C-Abrasive flow rate	0.1246	1	0.1246	7.48	0.0210
AB	0.0574	1	0.0574	3.45	0.0930
AC	0.0045	1	0.0045	0.272	0.6133
BC	1.290E-06	1	1.290E-06	0.0001	0.9932
A^2	0.0017	1	0.0017	0.1025	0.7555
B^2	0.0005	1	0.0005	0.0286	0.8690
C^2	0.0829	1	0.0829	4.98	0.0498
Residual	0.1666	10	0.0167		
Lack of fit	0.1280	5	0.0256	3.32	0.1071
Pure error	0.0386	5	0.0077		
Cor total	2.02	19			

which also confirms that the established model has high precision in predicting R_a and K_t .

Figure 6a-c display the response surface results of R_a . In Fig. 6a, the effect of the interaction between the stand-off distance and traverse speed on R_a is shown under the

Fig. 4 Residual plots of response **a** Surface roughness, **b** Kerf taper

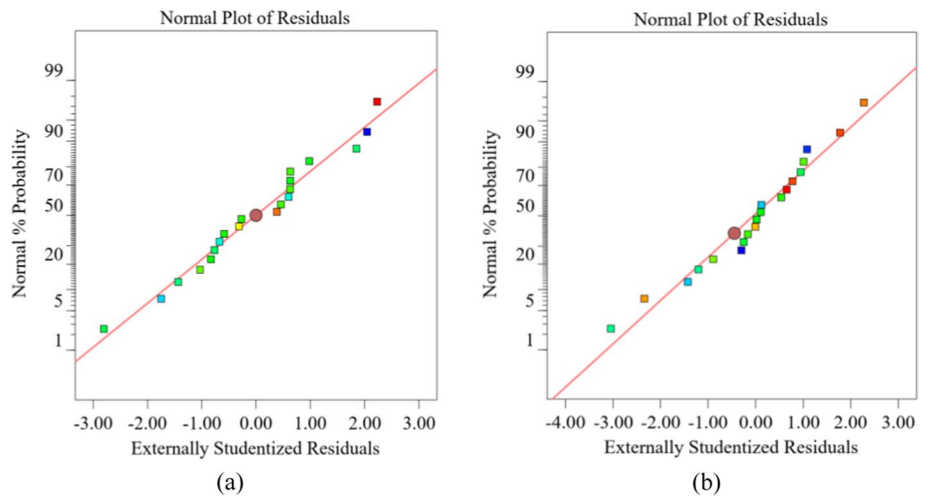


Fig. 5 Predicted versus Actual **a** Surface roughness, **b** Kerf taper

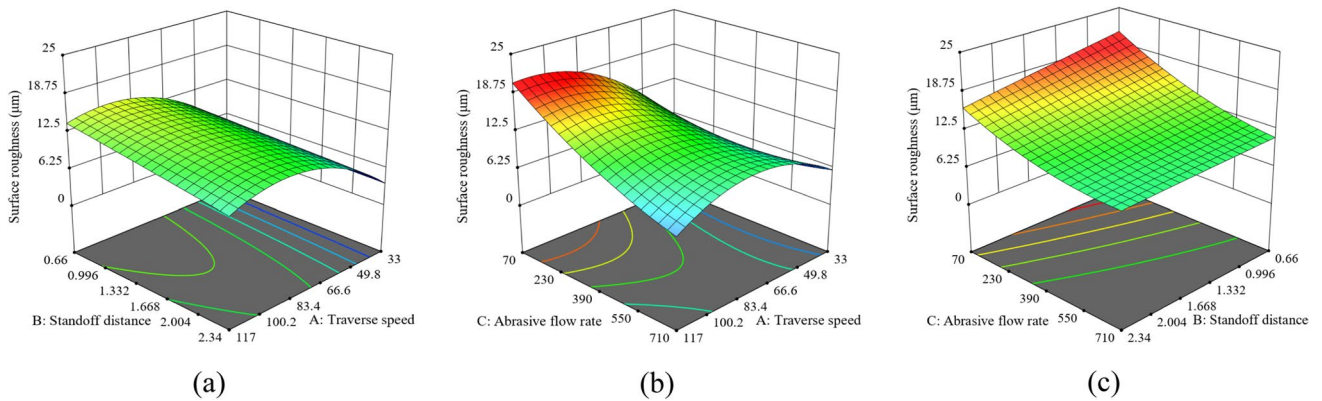
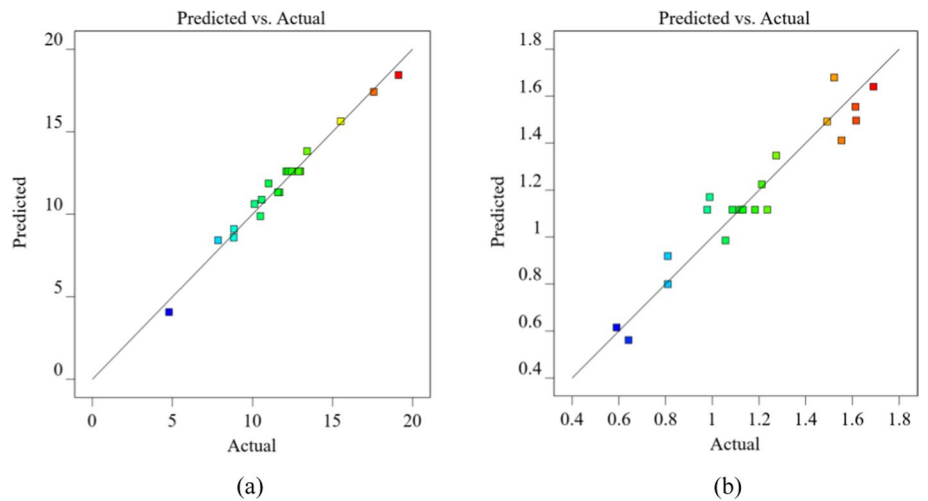


Fig. 6 3D response surface of surface roughness

abrasive flow rate of 390 g/min. For lower transverse speeds and higher standoff distances, the R_a will decrease. This is due to the reason that the cutting time of AWJ is increased [26]. The interaction between abrasive flow rate and traverse speed on R_a is shown in Fig. 6b, where the standoff distance remains unchanged at 1.5 mm. For a combination of a high abrasive flow rate and a low traverse speed, a decrease in R_a is observed. This is because the increase in abrasive flow rate increases the number of grits per unit time, which increases the cutting area of grits. As a consequence, the waterjet capacity is improved, making the processed surface cleaner [27]. Figure 6c is the 3D response surface of abrasive flow rate and standoff distance at a constant traverse speed of 75 mm/min. It can be seen that a smaller R_a can be obtained at an abrasive flow rate of 710 g/min and a standoff distance of 2.34 mm. This is because the increase in the standoff distance enlarges the acceleration time of AWJ and increases the grit kinetic energy, which in turn enhances the processing ability of AWJ.

Figure 7a-c portrays the 3D surface plot of the K_t with traverse speed, standoff distance, and abrasive flow rate. As can be seen from Fig. 7a, with the decrease in traverse speed and standoff distance, the K_t shows a decreasing trend. The minimum K_t can be obtained at the standoff distance of 0.66 mm and traverse speed of 33 mm/min. This is because the reduction in traverse speed increases the material removal time, resulting in similar kerf widths at the exit and entrance of the kerf. The reduction in the

target distance leads to the reduction in the diffusion angle of the AWJ, and the waterjet beam is concentrated in a smaller angular range [28]. Figure 7b and c shows that there is an intermediate abrasive flow rate of about 350 g/min that makes the K_t minimum. As the abrasive flow rate decreases, the contact between the grits also decreases. Thus, the kerf entrance and the kerf taper are decreased. However, an extremely low abrasive flow rate can lead to a sharp reduction in the AWJ’s cutting capability and the kerf width at the exit is small, resulting in a larger taper [29].

RSM is also an optimization method where the goal of optimization is to determine the optimal combination of parameters to obtain the optimal output response. The parameter optimization can achieve different optimization objectives, such as achieving the maximum or minimum value of the output response or achieving a specific target value. For multi-objective optimization, each optimization objective has a certain importance. The least important optimization goal is represented by (+), and the most important optimization goal is represented by (++ ++). Table 7 shows the relevant parameter optimization settings. In this study, the optimization process has two main objectives. Determine the minimum R_a and the minimum K_t for the cutting process using the maximum importance coefficient (++ ++), other parameters are normalized to find the combination of parameters that satisfies the objective proposal.

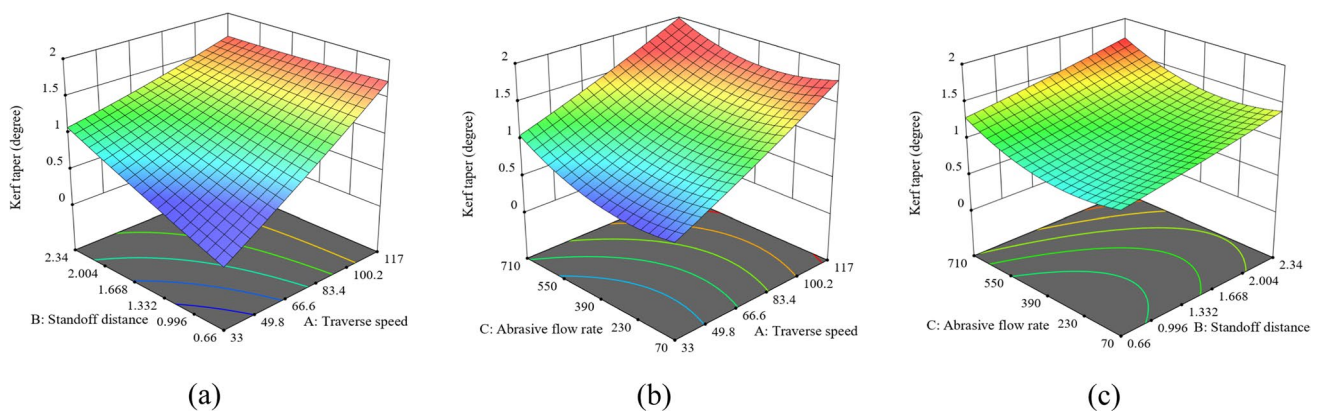


Fig. 7 3D response surface of kerf taper

Table 7 Parameter optimization settings

Name	Lower Limit	Upper Limit	Importance	Optimization Target
Traverse speed (mm/min)	33	117	+++	In range
Standoff distance (mm)	0.66	2.34	+++	In range
Abrasive flow rate (g/min)	70	710	+++	In range
R_a (μm)	0	20	+++++	Minimize
K_t (degree)	0	2	+++++	Minimize

The optimization results obtained based on the parameter optimization setting are $R_a=4.55 \mu\text{m}$ and $K_t=0.149^\circ$, with a corresponding expected value of 84.6% as shown in Table 8. At this time, the traverse speed is 33 mm/min, the standoff distance is 0.66 mm, and the abrasive flow rate is 339 g/min. Compared with the experimental results of the control group, R_a is reduced by 6.03%, and K_t is reduced by 86.67%.

3.2 Cutting quality improvement by the double-pass cutting strategy

In addition to the 20 specimens obtained at 150 MPa by single-pass cutting, another set of 20 specimens was also cut by 150 MPa double-pass cutting with alternate directions using the same cutting parameters. Then, using the optimal parameters obtained above, the specimens were cut by the two cutting strategies under the low-pressure waterjet condition, and the specimens of the high-pressure control group are shown in Fig. 8. It can be found that under 150 MPa single-pass cutting conditions, the presence of oblique stripes at the bottom of the cut surface can be seen in Fig. 8a. While under 350 MPa single-pass cutting, the trace of the stripe fades significantly and becomes a straight stripe. The reason is that the increase in pressure enhances its cutting ability and effective material removal can be achieved at the bottom

of the specimen as well. With 150 MPa double-pass cutting, the stripes are almost invisible on the cut surface, and the cut quality is even better than that of the 350 MPa cutting.

Specimens of run number 19 and the high-pressure control group were selected, and their surface morphology was measured using the NanoFocus μscan profiler as shown in Fig. 9, with a scanning frequency of 500 Hz and a resolution of $30 \mu\text{m} \times 30 \mu\text{m}$. As is demonstrated in Fig. 9a-c, the maximum height of the cutting surface in the Z-axis direction decreased from 118 to $98.4 \mu\text{m}$ by increasing the number of cuts, a reduction of 16.61%. Compared with the effect of high pressure cutting, the maximum height of 150 MPa double-pass cutting in the Z-axis direction is smaller than that of 350 MPa cutting.

Figure 10 shows the comparison of experimental data between single-pass cutting, double-pass cutting, and the dotted line shows the cutting results of the 350 MPa control group. From Fig. 10a, it can be observed that double-pass cutting can greatly reduce the R_a of the cut surface by a maximum of 82.74% (Run Number 14) while narrowing the difference between the R_a of the cut surface with different cutting parameters. Compared to the control group with 350 MPa cutting, double-pass cutting at low pressure can achieve better experimental results than the control group based on all combinations of the selected cutting

Table 8 Optimization results in R_a and K_t

Number	Traverse speed	Standoff distance	Abrasive flow rate	R_a	K_t	Desirability
1	33	0.66	339	4.55	0.149	0.846

Fig. 8 AWJ machined surface **a** 150 MPa single-pass cutting, **b** 150 MPa double-pass cutting, and **c** 350 MPa single-pass cutting

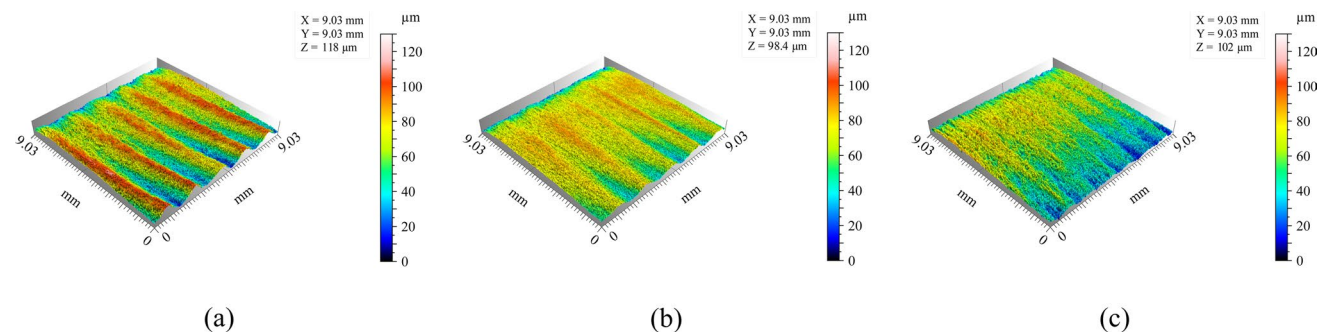
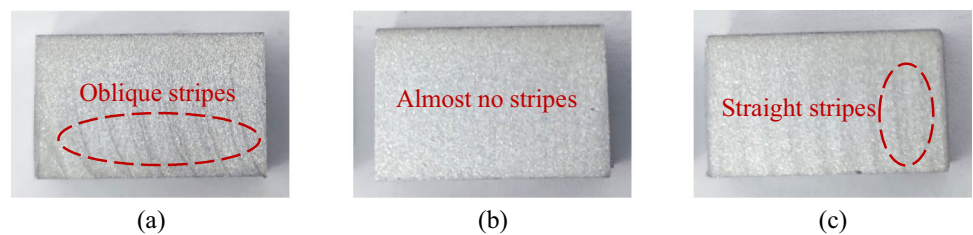


Fig. 9 Surface morphology produced by AWJ **a** 150 MPa single-pass cutting, **b** 150 MPa double-pass cutting, and **c** 350 MPa single-pass cutting

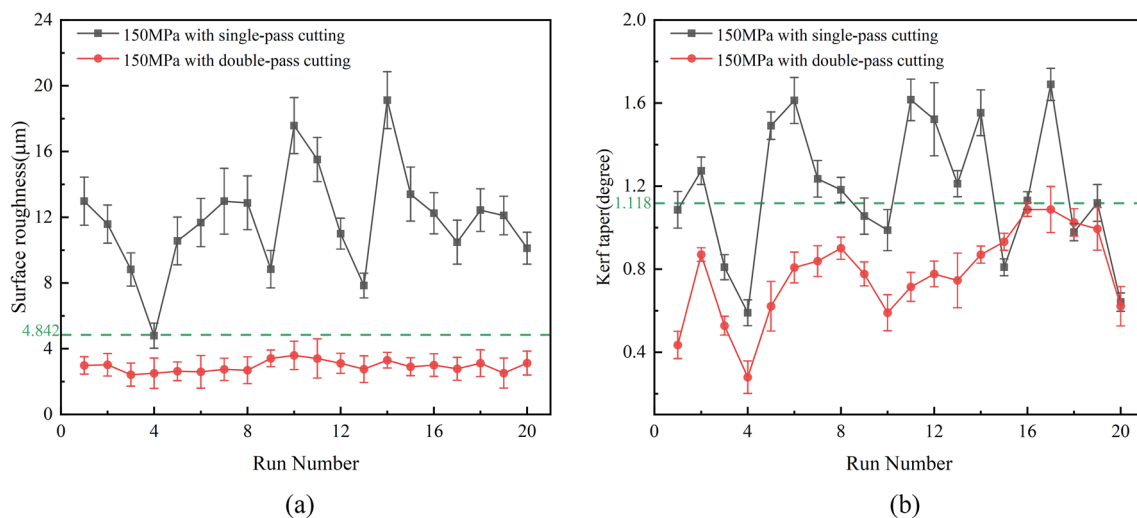


Fig. 10 **a** Surface roughness and **b** kerf taper under different cutting strategies.

parameters. Figure 10b displays the resulting curve for K_t , where the double-pass cutting similarly reduces the K_t by up to 59.94% (Run Number 1) compared to the single-pass cutting. When compared with the control group cutting, the K_t in the double-pass cutting mode in the low-pressure condition is also smaller than the control group in both cases. Therefore, the cut quality obtained under 350 MPa waterjet can be achieved by using the double-pass cutting method in 150 MPa condition.

In this study, the same traverse speed is used in single-pass cutting and double-pass cutting, so the machining efficiency of double-pass cutting is reduced. However, under the same cutting time, the cutting quality is still better than that of single-pass cutting when the traverse speed of double-pass cutting is increased. Therefore, the double-pass cutting strategy under low pressure can prolong the service life of the equipment without reducing the machining efficiency.

4 Conclusions

Although increasing the waterjet pressure is an effective and much direct way to promote the cutting quality of AWJ, the manufacturing, maintenance, and safety of the ultra-high-pressure pump are suffering great challenges. In the present study, the method for achieving high waterjet cutting quality at a relatively low pressure of 150 MPa was experimentally explored, and the main conclusions are as follows:

1. The experimental results show that reducing the traverse speed and standoff distance significantly reduces the R_a and K_t . In addition, increasing the abrasive flow rate decreases the R_a , while an optimal abrasive flow rate exists for the K_t .

2. The cut quality at the relatively low pressure of 150 MPa can be improved by optimizing the process parameters. The highest quality appears when the traverse speed is 33 mm/min, the standoff distance is 0.66 mm, and the abrasive flow rate is 339 g/min, where the R_a and K_t are reduced by 6.03% and 86.67%, respectively.
3. Double-pass cutting with alternate directions is an effective strategy for improving the cut quality at the relatively low pressure. After double-pass cutting, the R_a has reduced by a maximum of 82.74% and the greatest reduction in K_t is about 59.94%. The surface quality exceeded that of the high pressure cutting.

Funding This research is financially supported by the National Natural Science Foundation of China (No. 52175245) and the Natural Science Foundation of Hubei Province (No. 2021CFB462).

Declarations

Conflict of interest The authors declare that they have no competing financial interests or potential conflicts of interests with this research in this paper.

References

1. Natarajan Y, Murugesan PK, Mohan M, Khan SALA (2020) Abrasive Water Jet Machining process: a state of art of review. *J Manuf Processes* 49:271–322
2. Trivedi P, Dhanawade A, Kumar S (2015) An experimental investigation on cutting performance of abrasive water jet machining of austenite steel (AISI 316L). *Adv Mater Process Te* 1(3–4):263–274
3. Perc A (2018) Environmental aspects of abrasive water jet cutting. *Rocz Ochr Sr* 20:258–274

4. Llanto JM, Tolouei-Rad M, Vafadar A, Aamir M (2021) Recent progress trend on abrasive waterjet cutting of metallic materials: a review. *Appl Sci* 11(8):3344
5. Kumar A, Singh H, Kumar V (2018) Study the parametric effect of abrasive water jet machining on surface roughness of Inconel 718 using RSM-BBD techniques. *Mater Manuf Processes* 33(13):1483–1490
6. Joel C, Jeyapooan T (2021) Optimization of machinability parameters in abrasive water jet machining of AA7075 using Grey-Taguchi method. *Mater Today Proc* 37:737–741
7. Ahmed TM, El Mesalamy AS, Youssef A, Midany EI (2018) Improving surface roughness of abrasive waterjet cutting process by using statistical modeling. *CIRP J Manuf Sci Tec* 22:30–36
8. Natarajan Y, Murugasen PK, Sundarajan LR, Arunachalam R (2019) Experimental investigation on cryogenic assisted abrasive water jet machining of aluminium alloy. *Int J of Pr Eng Man-GT* 6:415–432
9. Xiong J, Wan L, Qian YN, Sun S, Li D, Wu SJ (2022) A new strategy for improving the surface quality of Ti6Al4V machined by abrasive water jet: reverse cutting with variable standoff distances. *Int J Adv Manuf Tech* 120:5339–5350
10. Yu Y, Sun T, Yuan Y, Gao H, Wang X (2020) Experimental investigation into the effect of abrasive process parameters on the cutting performance for abrasive waterjet technology: a case study. *Int J Adv Manuf Tech* 107:2757–2765
11. Kale A, Singh SK, Sateesh N, Subbiah R (2020) A review on abrasive water jet machining process and its process parameters. *Mater Today Proc* 26:1032–1036
12. Uthayakumar M, Khan MA, Kumaran ST, Slota A, Zajac J (2016) Machinability of nickel-based superalloy by abrasive water jet machining. *Mater Manuf Process* 31(13):1733–1739
13. Gnanavelbabu A, Rajkumar K, Saravanan P (2018) Investigation on the cutting quality characteristics of abrasive water jet machining of AA6061-B4C-hBN hybrid metal matrix composites. *Mater Manuf Process* 33(12):1313–1323
14. Karatas MA, Gokkaya H, Nalbant M (2020) Optimization of machining parameters for abrasive water jet drilling of carbon fiber-reinforced polymer composite material using Taguchi method. *Aircr Eng Aerosp Tec* 92(2):128–138
15. Wan L, Liu J, Qian YN, Wang XS, Wu SJ, Du H, Li D (2022) Analytical modeling and multi-objective optimization algorithm for abrasive waterjet milling Ti6Al4V. *Int J Adv Manuf Tech* 123(11):4367–4384
16. Qian YN, Xiong J, Li M, Chen W, Wu SJ, Wang XS, Li D (2023) Surface and profile treatment of China's U71Mn heavy rail using abrasive waterjet. *Int J Adv Manuf Tech* 124(7–8):2919–2930
17. Zhang J, Liu B, Lü R, Yang Q, Dai Q, (2020) Study on oil film characteristics of piston-cylinder pair of ultra-high pressure axial piston pump. *Processes* 8(1):68
18. Niu F, Tang B, Yue K, Liu D, Ma G, Wu D (2022) Effect of weaving frequency on pulsed laser weaving welding of thin 5052 aluminum alloy sheet. *Int J Adv Manuf Tech* 119(7–8):4541–4558
19. Guo N, Wu D, Wang G, Cheng Q, Fu Y, Yu M (2022) Investigation on underwater wire-feed laser deposition of 5052 aluminum alloy. *J Manuf Process* 76:687–694
20. Dong H, Tang Z, Li P, Wu B, Hao X, Ma C (2021) Friction stir spot welding of 5052 aluminum alloy to carbon fiber reinforced polyether ether ketone composites. *Mater Design* 201:109495
21. Kechagias JD, Fountas NA, Ninikas K, Petousis M, Vidakis N, Vaxevanidis N (2022) Surface characteristics investigation of 3D-printed PET-G plates during CO2 laser cutting. *Mater Manuf Process* 37(11):1347–1357
22. Iyer NP, Arunkumar N (2022) Investigation of abrasive water jet machining parameters of bismaleimide composites. *Mater Manuf Process* 37(14):1642–1651
23. Balamurugan K, Uthayakumar M, Sankar S, Hareesh US, Warriar KGK (2018) Effect of abrasive waterjet machining on LaPO4/Y2O3 ceramic matrix composite. *J Aust Ceram Soc* 54:205–214
24. Fuse K, Chaudhari R, Vora J, Patel VK, de Lacalle LNL (2021) Multi-response optimization of abrasive waterjet machining of Ti6Al4V using integrated approach of utilized heat transfer search algorithm and RSM. *Materials* 14(24):7746
25. Santhanakumar M, Adalarasan R, Rajmohan M (2016) Parameter design for cut surface characteristics in abrasive waterjet cutting of Al/SiC/Al2O3 composite using grey theory based RSM. *J Mech Sci Technol* 30:371–379
26. Deaconescu A, Deaconescu T (2021) Response surface methods used for optimization of abrasive waterjet machining of the stainless steel X2 CrNiMo 17–12-2. *Materials* 14(10):2475
27. Dumbhare AP, Dubey S, Deshpande VY, Andhare AB, Barve PS (2018) Modelling and multi-objective optimization of surface roughness and kerf taper angle in abrasive water jet machining of steel. *J Braz Soc Mech Sci Eng* 40:1–13
28. Santhanakumar M, Adalarasan R, Rajmohan M (2015) Experimental modelling and analysis in abrasive waterjet cutting of ceramic tiles using grey-based response surface methodology. *Arab J Sci Eng* 40:3299–3311
29. Selvam R, Karunamoorthy L, Arunkumar N (2017) Investigation on performance of abrasive water jet in machining hybrid composites. *Mater Manuf Process* 32(6):700–706

Publisher's Note Springer Nature remains neutral with regard to jurisdictional claims in published maps and institutional affiliations.

Springer Nature or its licensor (e.g. a society or other partner) holds exclusive rights to this article under a publishing agreement with the author(s) or other rightsholder(s); author self-archiving of the accepted manuscript version of this article is solely governed by the terms of such publishing agreement and applicable law.